

# Effect of drop-like aggregates on the viscous stress in magnetic suspensions

Modesto T Lopez-Lopez<sup>1</sup>, Pavel Kuzhir<sup>2</sup> and Andrey Zubarev<sup>3</sup>

<sup>1</sup>Departamento de Física Aplicada, Facultad de Ciencias, Universidad de Granada, Campus de Fuentenueva, 18071 Granada, Spain.

<sup>2</sup>Laboratoire de Physique de la Matière Condensée, Université de Nice-Sophia Antipolis – CNRS, Parc Valrose, 06108 Nice Cedex 2, Nice, France

<sup>3</sup>Urals Federal University, Lenina Ave 51, 620083, Ekaterinburg, Russia

E-mail: Andrey.Zubarev@usu.ru

Received:

## Abstract.

We present results of theoretical and experimental study of effect of dense drop-like aggregates on the magnetoviscous effects in suspensions of non-Brownian magnetizable particles. Unlike the previous works on this subject, we do not restrict ourselves by the limiting case of highly elongated drops. This allows us to reproduce the experimental rheological curve in wide region of the shear rate of the suspension flow.

Keywords: magnetorheological suspensions; drop-like aggregates; magnetoviscous effects.

## Introduction.

Suspensions of magnetizable particles in carrier liquids, so-called magnetorheological suspensions (MRS), attract considerable interest of investigators and engineers due to rich set of physical properties which find active applications in many modern and perspective high technologies. One of the most interesting and valuable, from the practical point of view, features of MRS is possibility to change, in a very broad range, their rheological properties and behavior under the action of quite moderate magnetic fields. The physical cause of the strong rheological effects is formation of heterogeneous structures (aggregates) composed of magnetic particles and aligned along with the applied field. Helpful reviews of the works on physics and practical applications of the magnetic suspensions can be found in [1-5].

In the quiescent suspensions, subjected to an external magnetic field, the aggregates can span the gap between the opposite walls of the flowing channel. In this state, MRS demonstrates elastic behavior with respect to the shear deformations. When the applied shear stress exceeds some threshold value (so-called static yield stress), the bonds between the aggregates and the walls are broken and the elastic regime changes to the viscous flow regime. In this regime, the measured macroscopical shear stress  $\sigma$  can be presented as

$$\sigma = \eta_0 \dot{\gamma} + \sigma_a \quad (1)$$

Here  $\eta_0$  is the viscosity of the carrier liquid,  $\dot{\gamma}$  is the macroscopic shear rate,  $\sigma_a$  is the stress produced by the aggregates. This stress is determined by the concentration, shape, length and orientation distribution of the aggregates.

Two kinds of the aggregates are usually considered. The first one is linear chains; the second kind of the aggregates is the dense bulk drops [1]. Theoretically, the effect of the chains on the stationary viscous properties of MRS with magnetizable particles has been studied in refs. [6,7].

The effect of the bulk “drops”, consisting of great number of particles, has been studied in refs. [8, 9]. The model [8] is based on minimization of the magnetic (electrical) free energy of a magnetizable (polarizable) ellipsoidal drop tilted with respect to the applied field. Analysis [8] has been done for highly elongated drops and leads to the following scaling relation:

$\sigma_a \propto \dot{\gamma}^{1/3} H_0^{4/3}$ , where  $H_0$  is the magnetic field inside the suspension. It should be noted that the approach of the ref. [8] does not take into account any mechanisms of the drop destruction by the hydrodynamic viscous forces. Analysis shows that consideration of these mechanisms is principally important for development of a physically correct theory of rheological properties of suspensions with the heterogeneous aggregates.

The rupture of particles from the aggregated surface by the viscous forces has been considered in [9]. This model leads to the relation,  $\sigma_a \propto H_0^2$ ; like in the chain model [6], the stress,  $\sigma_a$ , does not depend on the shear rate  $\dot{\gamma}$ . The model [9] is often used for the interpretation of rheological effects in the magnetic suspensions (see overview in ref.[1]). However, this model contains a parameter (the thickness of a gap between the particles in the aggregates) which is not determined theoretically and is considered as a fit parameter of the model. Strictly speaking, the interparticle gap thickness must depend both on the field  $H_0$  and the shear rate  $\dot{\gamma}$ , however in [9] this thickness is considered as a constant. Analysis shows that dependence of the gap thickness on the shear rate leads to qualitative change of the dependence of  $\sigma_a$  on  $\dot{\gamma}$ . Therefore, the results of [9] require very cautious attitude.

Like in ref.[8], the model [9] deals with the limiting approximation of the highly elongated aggregates. However this approximation is not valid when the shear rate  $\dot{\gamma}$  is large enough and too long aggregates are destroyed by the viscous forces.

We present here results of theoretical study of effect of the bulk drops on the magnetoviscous effects in MRS with the linearly magnetizable particles. The model is based on the analysis of hydrodynamic destruction forces acting on the aggregate surface and does not contain any adjustable parameters. It should be noted that appearance of the bulk drops has been observed in many experiments and computer simulations of magnetic suspensions (see, for example, overview in [1]).

In the framework of this model we suppose that the drop size is significantly less than the width of the flow channel (the case of the developed flow) and effect of the channel walls on the drop behavior is negligible. The validity of this assumption will be proved at the end of the paper. Unlike refs [8,9] we do not restrict ourselves by the asymptote of the highly elongated drops. It allows us to reproduce the suspension rheograms in the wide range of the shear rates,  $\dot{\gamma}$ .

### **Main approximations.**

Let us consider a dense aggregate consisting of the large number of magnetizable particles. We will model the aggregate by an ellipsoid of revolution with the major and minor axes  $a$  and  $b$ , respectively. These magnitudes will be estimated below. We suppose that the suspension is subjected to a macroscopic shear flow with the rate  $\dot{\gamma}$ . When  $\dot{\gamma} = 0$ , the aggregate major axis is aligned along the magnetic field  $\mathbf{H}_0$ . Under the shear hydrodynamic forces, the ellipsoid axis deviates from the field by the angle  $\theta$ . We will suppose that the field  $\mathbf{H}_0$  is applied in the direction of gradient of the flow velocity. Next, we suppose that concentration of the drops in the suspension is small enough and any interactions between them can be ignored. The validity of

this assumption will be reconsidered at the end of the paper. The problem geometry is illustrated in Fig.1.

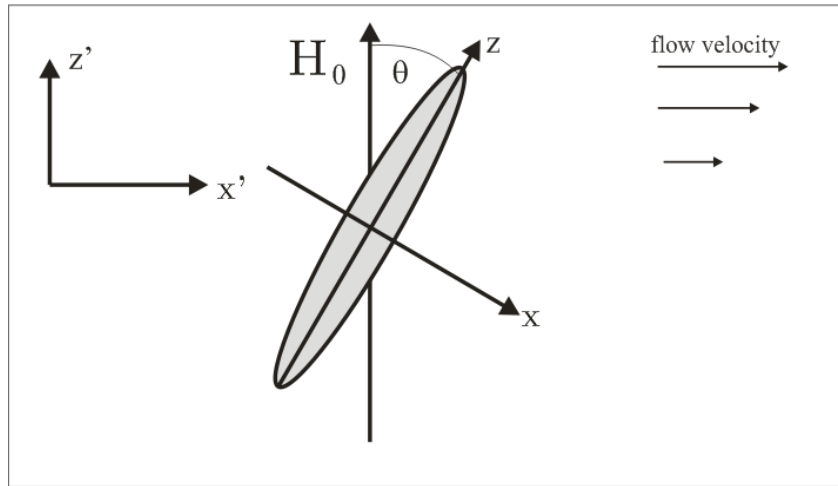


**Fig.1.** Sketch of the model of the drop-like aggregates. The horizontal arrows illustrate the suspension macroscopic flow.

Macroscopic stress  $\sigma_a$  is determined by the shape of the drops and the angle  $\theta$  of the drop inclination with respect to the field direction. On the other hand, the angle  $\theta$  is determined by the hydrodynamic and magnetic torques acting on the aggregate; while the size and shape of the drop is defined by the combination of the hydrodynamic and magnetic forces acting on the drop surface. The magnetic force consists of the elongating force of the demagnetizing field along with the force of the surface tension. Obviously, the surface tension force tends to contract the drop. Our aim is to estimate the angle  $\theta$  as well as the hydrodynamic and magnetic forces, and then – the size and the shape of the steady stable drop in the suspension under applied shear flow. For the maximal simplification of calculations we will consider this aggregate as a rigid ellipsoid, impenetrable for the carrier liquid, and restrict our analysis to a linear law of the particles magnetization.

### The orientation angle $\theta$ .

The magnetic torque  $\Gamma_m$ , acting on the ellipsoidal drop, can be found, for example, in the book [10] (see, also, [8,9]) as:

$$\Gamma_m = \frac{1}{2} V \mu_0 \frac{\chi^2 (1-3N)}{(1+N\chi)(2+(1-N)\chi)} H_0^2 \sin 2\theta \quad (2)$$

Here  $V = \frac{4}{3} \pi a b^2$  is the aggregate volume,  $\mu_0$  is the magnetic permeability of vacuum,  $\chi$  is the aggregate magnetic susceptibility,  $N$  is the aggregate demagnetizing factor in the direction of the main axis  $a$ . The explicit form of this factor can be found, in [10].

The hydrodynamic torque  $\Gamma_h$  has been calculated in ref. [11] (see, also, [8]) as:

$$\Gamma_h = V \eta_0 \dot{\gamma} \frac{4}{2r^2 N + 1 - N} (r^2 \cos^2 \theta + \sin^2 \theta) \quad (3)$$

Here  $r=a/b$  is the drop aspect ratio, which will be determined below.

Equating the torques  $\Gamma_h$  and  $\Gamma_m$ , we get:

$$\tan \theta = \frac{BMa^{-1} - \sqrt{B^2Ma^{-2} - 4AC}}{2A}, \quad (4)$$

where  $Ma = \frac{\eta_0 \dot{\gamma}}{\mu_0 H_0^2}$  is the Mason number characterizing a ratio of the hydrodynamic-to-magnetic forces acting on aggregates,

$$A = \frac{4}{2r^2N + 1 - N}, \quad B = \frac{\chi^2(1-3N)}{(1+N\chi)(2+(1-N)\chi)}, \quad C = \frac{4r^2}{2r^2N + 1 - N}$$

### Hydrodynamic destructing forces

We will estimate now a hydrodynamic force, which tends to elongate and, finally, to break the drop in the direction of the main axis  $a$ .

Let us introduce the Cartesian coordinate systems with the axes  $Oz'$  and  $Ox'$ , aligned along the gradient of the suspension velocity (i.e. along the field  $\mathbf{H}_0$ ) and along the velocity respectively; we also introduce another reference frame with the axes  $Oz$  along the major axis of the drop and the axis  $Ox$  situated in the plane  $Ox'z'$ . Both these coordinate systems are shown in Fig.1.

In the laboratory ( $Ox'z'$ ) frame the components of the flow velocity read:

$$v_{x'} = \dot{\gamma}z', \quad v_{y'} = v_{z'} = 0 \quad (5)$$

By using the standard formulas for transformations of vector components from one coordinate system to another, one can easily find the velocity components in the reference frame  $Oxz$ . After that we can determine the components of the rate-of-strain tensor in this frame:

$$\gamma_{xz} = \frac{1}{2} \left( \frac{\partial v_x}{\partial z} + \frac{\partial v_z}{\partial x} \right) = \frac{1}{2} \dot{\gamma} (\cos^2 \theta - \sin^2 \theta), \quad (6)$$

$$\omega_{xz} = \frac{1}{2} \left( \frac{\partial v_x}{\partial z} - \frac{\partial v_z}{\partial x} \right) = \frac{1}{2} \dot{\gamma} = -\omega_{zx}$$

$$\gamma_{zz} = \frac{\partial v_z}{\partial z} = \dot{\gamma} \sin \theta \cos \theta,$$

$$\gamma_{xx} = \frac{\partial v_x}{\partial x} = -\dot{\gamma} \sin \theta \cos \theta$$

All remaining components of this tensor are zero.

The viscous force, acting on the unit area of the drop surface, has been estimated in ref. [12]. The component of this force, acting in  $z$  direction (i.e. along the major axis  $a$  of the drop), can be presented in the form:

$$P_z = \eta_0 S \left( \left( \frac{8}{ab^2} A_{zz} - 4W \right) \frac{z}{a^2} + \frac{8}{ab^2} A_{xz} \frac{x}{b^2} \right) \quad (7)$$

$$S = \left( \frac{x^2 + y^2}{b^4} + \frac{z^2}{a^4} \right)^{-1/2}$$

$$W = \alpha_0 A_{zz} + \beta_0 (A_{xx} + A_{yy})$$

$$A_{zz} = \frac{2\alpha_0'' \gamma_{zz} - \beta_0'' \gamma_{xx}}{6((\beta_0'')^2 + 2\alpha_0'' \beta_0'')} \quad A_{xz} = \frac{\beta_0 (a^2 - b^2)}{2(\beta_0 - \alpha_0)(b^2 \beta_0 + a^2 \alpha_0)} \gamma_{xz} + \frac{a^2}{2(b^2 \beta_0 + a^2 \alpha_0)} \omega_{xz}$$

$$A_{yy} = -\frac{\alpha_0''\gamma_{zz} + \beta_0''\gamma_{xx}}{6((\beta_0'')^2 + 2\alpha_0''\beta_0'')}$$

Here  $x, y, z$  are coordinates of a point on the drop surface. The following obvious relation describing the aggregate surface holds:

$$\frac{z^2}{a^2} + \frac{x^2 + y^2}{b^2} = 1 \quad (8)$$

Parameters  $\alpha_0, \beta_0, \alpha_0'', \beta_0''$  depend on the aggregate aspect-ratio  $r$ ; their explicit forms are given in the Appendix I.

Integral of  $P_z$  over the whole surface of the drop means the total force acting on the drop in the shear flow. One can easily see that this integral is equal to zero, as it should be for force-free aggregates. The hydrodynamic force  $f_h$ , stretching the drop in  $z$  direction, equals to the integral from  $P_z$  over a half of the surface, say, corresponding to  $z > 0$ .

After calculations (see Appendix II) we get:

$$f_h = \eta_0 4\pi \left( \frac{2}{ab^2} A_{zz} - W \right) b^2 \frac{r^2}{r^2 - 1} \left[ 1 + \frac{1}{r\sqrt{r^2 - 1}} \ln(r - \sqrt{r^2 - 1}) \right] \quad (9)$$

### Magnetic forces.

The magnetic force, which determines the shape of the aggregate, can be determined as:

$$f_m = -\frac{\partial F_m}{\partial a} \quad (10)$$

where  $F_m$  is the magnetic free energy of the drop. This energy can be written in the following form:

$$F_m = F_b + F_s \quad (11)$$

Here  $F_b$  is the bulk free energy of the drop, determined by the effects of the drop demagnetizing field,  $F_s$  is the surface tension free energy.

The bulk free energy can be presented as (see, for example [13]):

$$F_b = -\frac{\mu_0}{2} V \chi \left( \frac{\cos^2 \theta}{1 + \chi N} + \frac{2 \sin^2 \theta}{2 + \chi(1 - N)} \right) H_0^2$$

The surface free energy is:

$$F_s = \int \sigma_s ds$$

Here  $\sigma_s$  is the coefficient of the surface tension,  $ds$  is an infinitesimal element of the drop surface. Strictly speaking,  $\sigma_s$  depends on the position of a point on this surface. This fact makes all calculations very complicated and cumbersome. For maximal simplification of the calculations, we will estimate  $F_s$  as:

$$F_s = \xi \Sigma \quad (12)$$

Here  $\xi$  is the surface tension coefficient, averaged over the drop surface,  $\Sigma$  is the surface area. For the prolate ellipsoid of revolution the area can be calculated as:

$$\Sigma = 2\pi \left( \frac{3V}{4\pi} \right)^{2/3} r^{-2/3} \left( 1 + r^2 \frac{\arcsin \sqrt{1-r^{-2}}}{\sqrt{r^2-1}} \right) \quad (13)$$

The stretching force  $f_b$ , corresponding to the free energy  $F_b$ , is:

$$f_b = -\frac{\partial F_b}{\partial a} \Big|_{V,\theta} = -\frac{\partial F_b}{\partial r} \Big|_{V,\theta} \frac{\partial r}{\partial a} \Big|_V = \frac{\mu_0}{2} V \chi^2 \left[ \frac{\cos^2 \theta}{(1+\chi N)^2} - \frac{2 \sin^2 \theta}{(2+\chi(1-N))^2} \right] \frac{\partial N}{\partial r} \frac{3}{2} \left( \frac{4\pi}{3V} \right)^{1/3} r^{1/3} H_0^2 \quad (14)$$

The average coefficient of the surface tension can be estimated as (see, Appendix III):

$$\xi \approx \frac{\mu_0}{4} \chi H_0^2 \left[ \left( \frac{\cos \theta}{1+\chi N} \right)^2 + \left( \frac{2 \sin \theta}{2+\chi(1-N)} \right)^2 \right] \delta \quad (15)$$

Here  $\delta$  is the thickness of the interface zone between the dense drop and the dilute environment. In the order of magnitude, this thickness equals to the particle diameter (see, for example, [8]). The force of the surface tension is:

$$f_s = -\frac{\partial F_s}{\partial a} \Big|_{V,\theta} = -\frac{3}{2} \frac{\partial F_s}{\partial r} \left( \frac{4\pi}{3V} \right)^{1/3} r^{1/3} \quad (16)$$

The explicit form of  $f_s$  is cumbersome and we omit it here for brevity.

The shape of the steady stable drop is determined from the condition that the total deforming force  $f$ , acting on the drop surface, is zero. Substituting  $\theta$  from (4) into eqs. (9,14,16), we get:

$$f(V, r) = f_h(V, r) + f_b(V, r) + f_s(V, r) = 0 \quad (17)$$

The second equation, necessary for calculation of two variations  $V$  and  $r$ , can be found from the following considerations. The plots of the force  $f$ , as a function of the aspect ratio  $r$ , for three magnitude of the volume  $V$  are shown in Fig.2.

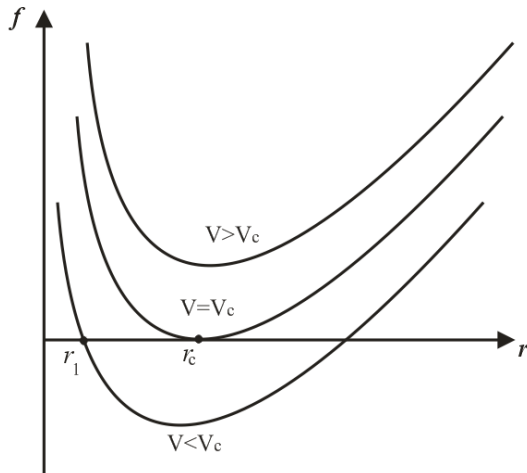


**Fig.2.** Illustration of dependence of the deformation force  $f$  vs. the drop aspect ratio  $r$ .

The positive magnitudes of  $f$  correspond to the drop elongation along the major axis  $a$ ; the negative ones – to the drop contraction. If  $V > V_c$ , the force stretches the drop until it breaks; this happens at all magnitudes of the aspect ratio  $r$ . Therefore, the aspect ratio  $r_c$  and the volume  $V_c$  of the stable drop are determined as solutions of the systems of equation (17) and the equation

$$\frac{\partial f(V, r)}{\partial r} = 0 \quad (18)$$

The system (17),(18) can be easily solved numerically.

### Magnetoviscous stress $\sigma_a$ .

In the first approximation the stress  $\sigma_a$ , produced by the magnetizable aggregates, can be estimated as (see, for example, [8,9] and references there):

$$\sigma_a = \frac{1}{2} n_a \Gamma_m$$

where  $n_a$  is the number of the aggregates in a unit volume of the system.

By using here the relation (2), one can get

$$\sigma_a = \frac{1}{4} \Phi \mu_0 \frac{\chi^2 (1 - 3N(r))}{(1 + N(r)\chi)(2 + (1 - N(r))\chi)} H_0^2 \sin 2\theta \quad (19)$$

Here  $\Phi = n_a V$  is the volume concentration of the aggregates. Estimates show that for a magnetic field strength  $H_0$  as low as 1 kA/m, the energy of the magnetic interaction between the particles is much higher than the thermal energy  $kT$ . In this case, all the particles must be condensed into the domains (drops) of dense phase and we get:

$$\Phi = \frac{\varphi_0}{\varphi_a}$$

where  $\varphi_0$  is the total volume concentration of the particles in the suspension,  $\varphi_a$  is the particle volume concentration in the drop.

In the dense aggregate this concentration can be estimated as  $\varphi_a \approx 0.6 - 0.7$ . We find the stress  $\sigma_a$  by substitution of Eq. (4) for  $\theta$  and the solution of Eqs. (17), (18) into the expression (19). Predictions of the theoretical model for the total stress  $\sigma$  are compared with experimental results in Fig. 3. Details of experimental methods are given in Appendix IV. Note that the stress  $\sigma$  does not depend on the parameter  $\delta$  of the drop surface tension. This follows both from the general dimensional analysis, as well as from the solution of the system (17,18).

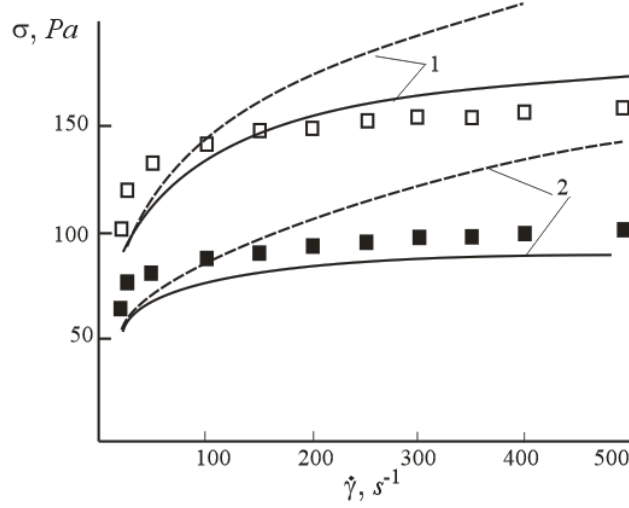


**Fig.3** Total stress  $\sigma$  vs. the shear rate  $\dot{\gamma}$ . Lines represent theoretical predictions and dots the experimental data. Solid lines - calculations with (17-19), the dashed ones – by using the asymptotic estimate (20). Line 1 and open squares correspond to  $H_0=8.6$  kA/m; line 2 and black squares - to  $H_0=5.7$  kA/m. Parameters of the systems:  $\varphi_0=0.1$ ;  $\varphi_a=0.65$ ;  $\chi=85$ ;  $\eta_0 = 5$  mPa·s.

As observed in Figure 3 there is a quite good correspondence between theory and experiments. This agreement shows that the observed magnetorheological effects can be explained by appearance of the drop-like aggregates and that the suggested model is adequate, at least, in its main points.

Estimates show that, for small Mason numbers  $Ma \ll 1$ , the aspect ratio  $r \gg 1$  and the general solution (19) shows the following asymptotic behavior:

$$\sigma_a \approx \Phi(\mu_0 H^2)^{2/3} (\eta_0 \dot{\gamma})^{1/3} \kappa, \quad \kappa = \left[ \frac{7}{22} \frac{\chi^4}{(2 + \chi)} \right]^{1/3} \quad (20)$$

It should be noted that the same scaling relation  $\sigma_a \propto H^{4/3} \dot{\gamma}^{1/3}$  has been obtained in [8] from the energetic considerations, discussed in Introduction of the present paper. However the relation (20) corresponds to experimental situation only when the shear rate  $\dot{\gamma}$  are small enough. For large magnitudes of  $\dot{\gamma}$ , the asymptotic relation (20) overestimates the experimental results and the disagreement between theory and experiments increases with  $\dot{\gamma}$ . The relation (19) can be applied in much more wide region of  $\dot{\gamma}$  than (20).

Let us now analyze briefly the range of validity of our model. Firstly, our model is valid for the shear rates higher than some critical value corresponding to the maximum length of the aggregates when they become gap-spanning. This length is easily calculated under the asymptote of low shear rates, or equivalently, low Mason numbers giving the flowing expression for the critical Mason number:  $Ma_c = \kappa^{3/2} \ln^{1/2} \vartheta / (3^{1/2} \vartheta)$ , where  $\vartheta = 72 \chi^2 g / (11 \pi \delta)$  and  $g$  is the flow channel thickness corresponding to the rheometer gap in our experiments. For the typical set of the parameters appropriate to our experiments (gap thickness,  $g=0.35$  mm, transition layer  $\delta=0.5$   $\mu\text{m}$  between the bulk aggregates and the surrounding medium, aggregate magnetic susceptibility,  $\chi \approx 85$ , and magnetic field intensity  $H_0=5.7-8.6$  kA/m), we obtain the following estimate for the critical Mason number and the critical shear rate above which our model is considered to be valid:  $Ma_c \sim 10^{-4}$  and  $\dot{\gamma} \sim 1 \text{ s}^{-1}$ . Thus, in our experiments, focused on the developed flow regime at relatively high shear rates ( $1 < \dot{\gamma} < 500 \text{ s}^{-1}$ ), the aggregates are not expected to span the gap, and the present model could be applied safely.



Secondly, it should be noted that we ignored hydrodynamic interactions between the drop-like aggregates. Obviously, in suspensions with high enough concentrations of the particles  $\varphi_0$  and, therefore, high concentration of drop-like aggregates,  $\Phi$ , both hydrodynamic and magnetic interactions between the drops can, in principle, be significant. However analysis shows that in suspensions of elongated particles (drop-like aggregates in our case), the effect of the hydrodynamic interaction is weak as compared to the effect of the interaction between the flow and individual particles [20, 21]. It is commonly recognized that the stress in the semi-diluted fiber suspensions differs only modestly from that in the diluted ones [22]. Furthermore, in concentrated suspensions of rod-like particles the short-range hydrodynamic interactions between particles become significant only at concentrations respecting the condition  $\Phi \sin \Theta \geq 10^{-1}$  [23], with  $\Theta$  being the average angle between axes of neighboring particles. In the case of strongly oriented drop-like aggregates, the angle  $\Theta$  appears to be much smaller than unity ( $\Theta \ll 1$ ), and the short-range hydrodynamics should not play any significant role on the stress level.

Thirdly, magnetic interaction between the drops can also affect the magnetic force and torque acting on each drop, as well as the macroscopic suspension stress. A simple estimate of the effect of the neighboring aggregates on the magnetic torque acting on a given aggregate can be obtained using the Maxwell-Garnett mean field theory [24] applied to the limit of low Mason numbers, thus high aggregate aspect ratios  $r \gg 1$ . At this condition, the aggregate demagnetization factor vanishes,  $N \approx 0$ , and the fraction in Eq. 2 for the magnetic torque reduces to  $\chi^2(1-\Phi)/(2+(1-\Phi)\chi)$  if the magnetic interactions between aggregates are taken into account, instead of  $\chi^2/(2+\chi)$  if the interactions are ignored. For the aggregates of high magnetic permeability,  $\chi \approx 85$  (as the ones composed of iron particles - our experimental case), the difference between both estimates is only a few percent. Thus, inter-aggregate magnetic interactions are not expected to enhance considerably the magnetic torque and the suspension stress, and the relationships (2) and (19) ignoring these interactions may still be applied.

In summary, we believe that the assumption of negligible inter-aggregate interactions is justified for the MR suspensions used in our experiments having a particle volume fraction up to 10%. The quantitative agreement between the theoretical and experimental results supports this assumption. Extension of the present theory to a broader concentration range, where interactions between the drops cannot be more ignored, could be a natural generalization of the present model.

## Conclusion

Results of theoretical study of magnetoviscous effects in magnetorheological suspensions with the drop-like aggregates are presented. The analysis is done beyond the standard asymptotic simplification of extremely elongated drops. We suppose that in the shear flowing suspension the volume and shape of the stable drop is determined by the balance between the hydrodynamic and magnetic forces which tend, respectively, to elongate and contract the drop in the direction of its main axis. The theoretical results are in agreement with the experiments in a wide region of shear rate of the suspension flow, whereas the standard asymptotic estimates correspond to the experiments only when the shear rate is small enough.

## Acknowledgment

This work has been supported by the Russian Fund of Fundamental Investigations, grants 12-01-00132, 13-02-91052, 13-01-96047, 14-08-00283; by the Act 211 Government of the Russian Federation № 02.A03.21.0006; by the Junta de Andalucía (Spain), project P09-FQM-4787; and by the University of Granada (Acción Integrada con Russia; Plan Propio 2011); and CNRS PICS N° 6102 is also acknowledged.

## Appendix I.

The kinetic coefficients  $\alpha_0, \dots, \beta_0''$ , determined in [12] (see, also, [14]), read:

$$\alpha_0 = -\frac{b^{-3}}{r^2 - 1} \left[ \frac{2}{r} + \frac{1}{\sqrt{r^2 - 1}} \ln(2r^2 - 1 - 2r\sqrt{r^2 - 1}) \right],$$

$$\beta_0 = \frac{b^{-3}}{r^2 - 1} \left[ r - \frac{1}{2\sqrt{r^2 - 1}} \ln(2r^2 - 1 + 2r\sqrt{r^2 - 1}) \right],$$

$$\alpha_0'' = \frac{b^{-3}}{4(r^2 - 1)^2} \left[ r(2r^2 + 1) - \frac{4r^2 - 1}{2\sqrt{r^2 - 1}} \ln(2r^2 - 1 + 2r\sqrt{r^2 - 1}) \right],$$

$$\beta_0'' = -\frac{b^{-3}}{(r^2 - 1)^2} \left[ 3r + \frac{2r^2 + 1}{2\sqrt{r^2 - 1}} \ln(2r^2 - 1 - 2r\sqrt{r^2 - 1}) \right].$$

## Appendix II. Calculation of the hydrodynamic deformation force $f_h$ .

For calculation of the force  $f_h$  we will introduce the cylindrical coordinate systems  $(z, \rho, \psi)$  according to the rule:  $z = z, x = \rho \cos \psi, y = \rho \sin \psi$ . The following relation applies for the ellipsoid surface:

$$\rho(z) = b \sqrt{1 - \frac{z^2}{a^2}}$$

The force  $f_h$  reads:

$$f_h = \int_0^a \left( \int_0^{2\pi} P_z d\psi \right) \rho(z) dz = 2\pi\eta_0 \dot{\gamma} \left( \frac{8}{ab^2} A_{zz} - 4W \right) a^{-2} b \int_0^a \frac{\rho(z)z}{\left( \frac{\rho(z)^2}{b^4} + \frac{z^2}{a^4} \right)^{1/2}} dz \quad (\text{A.1})$$

The last integral can be presented as:

$$\int_0^a \frac{\rho(z)z}{\left( \frac{\rho(z)^2}{b^4} + \frac{z^2}{a^4} \right)^{1/2}} dz = \frac{b^2}{2} \int_0^1 \frac{\sqrt{1-s}}{\sqrt{1-\beta s}} ds = \frac{b^2}{2\beta} \left[ 1 + \frac{1-\beta}{\sqrt{\beta}} \ln \frac{1-\sqrt{\beta}}{\sqrt{1-\beta}} \right], \quad \beta = 1 - r^{-2} \quad (\text{A.2})$$

Substituting (A.1) into (A.2) we come to the relation (9).

## Appendix III. Estimate of the mean surface tension $\xi$ .

By using the definition of the surface tension [15], we can estimate the coefficient of the surface tension as

$$\sigma_s \propto -\frac{1}{2} \Psi_m \delta \quad (\text{A.3})$$

Here  $\delta$  is thickness of the transition zone between the phase of the dense droplet and the dilute environment,  $\Psi_m$  is the density of the free energy of magnetic interaction between particles in the dense drop. The last magnitude is:

$$\Psi_m = -\frac{\mu_0}{2} \chi H^2 \quad (\text{A.4})$$

where  $H$  is magnetic field inside the drop. The Cartesian components of this field in the coordinate system  $Oxz$ , shown in Fig.1, can be written down as (see, for example, [10]):

$$H_z = \frac{1}{1 + \chi N} H_0, \quad H_x = \frac{2}{2 + \chi(1 - N)} H_0 \quad (\text{A.5})$$

Obviously  $H^2 = H_x^2 + H_z^2$ .

The thickness  $\delta$  of the transition layer between the droplet and surrounding medium depends on the position of a point on the droplet surface. Its calculation presents very sophisticated problem of statistical physics of the interface zone. For dense drops with the concentration of particles near the concentration of the dense packing, the thickness  $\delta$  is of the order of magnitude of the particle diameter  $d$ . In the approximation that  $\delta$  is constant and does not depend on the position on the droplet surface, we replace in (A.3)  $\sigma_s$  to  $\xi$ . Combining (A.3)-(A.5), we come to the estimate (12,15).

#### Appendix IV. Experimental methods.

Iron powder (HQ quality; density  $7.5 \text{ g} \cdot \text{cm}^{-3}$ ) supplied by BASF (Germany) was used as magnetic phase for the preparation of the MRS. SEM pictures revealed that this powder consisted of spherical particles with 930 nm of average diameter and 330 nm of standard deviation [16]. Kerosene (viscosity  $2.1 \text{ mPa} \cdot \text{s}$ ; density  $0.79 \text{ g/cm}^3$ ) supplied by Sigma-Aldrich (Germany) was used as carrier liquid. Clay particles (Claytone HY), supplied by Southern Clay Products, Inc. (Texas, USA) were used as stabilizing (thickening) agent in order to hinder the settling of the iron particles. In the developed shear flow regime, the viscosity of the clay-kerosene mixture was  $5 \text{ mPa} \cdot \text{s}$ . Iron suspensions were prepared as described in Ref. [17] and had a final iron particle volume concentration of 10 %. Previous experiments showed that at low field, the relative magnetic susceptibility  $\chi_p$  of the iron powder is approximately independent of the field and takes an approximate value  $\chi_p = 130$  [18]. Thus, the susceptibility of the drop with the densely packed particles can be roughly estimated as  $\chi \sim \chi_p \phi_p$  [19]. By using  $\phi_p \sim 0.65$ , we have the estimate  $\chi \sim 85$ .

Rheological measurements were performed in a controlled rate mode using a MCR 300 Physica-Anton Paar magnetorheometer at  $25 \text{ }^\circ\text{C}$ . The measuring system geometry was a 20 mm diameter parallel-plate set for a gap width of 0.35 mm.

#### References

- [1] G. Bossis, O. Volkova, S. Laciš, A. Meunier 2002 Lectures Notes in Physics, 594, 201.
- [2] S. Odenbach (Ed), Colloidal Magnetic Fluids (Berlin, Springer, 2009)
- [3] S. Odenbach, Magnetoviscous Effects in Ferrofluids (Berlin, Springer, 2002)
- [4] J. M. Ginder, MRS Bull., 23 (1998) 26
- [5] J. K. de Vicente, D. J. Klingenberg, R. Hidalgo-Álvarez, Soft Matter 7 (2011) 3701
- [6] J. E. Martin, R. Anderson, J.Chem.Phys., 104 (1996) 4814
- [7] A.Yu. Zubarev. L.Yu. Iskakova, Physica A 382 (2007) 378.
- [8] T.Halsey, J. Martin, D. Adolf, Phys. Rev. Letters, 68, (1992) 1519
- [9] Z. P. Shul'man, V. I. Kordonskii, E. A. Zal'tsgendler, I.V.Prokhorov, B.M. Khusid, S.A.

- Demchuk, *Magnetohydrodynamics* 20, (1984) 354; V.I. Kordonsky, Z. P. Shulman, S.R. Gorodkin, S.A. Demchuk, I.V. Prokhorov, E.A. Zaltsgendler, B.M. Khusid, *J. Magn. Magn. Materials*, 85 (1990) 114
- [10] L.D. Landau, E.M. Lifshits, *Electrodynamics of Continuous Media* (London, Pergamon Press, 1960)
- [11] G.B. Jeffery, *Prog. Roy. Soc. A* 102 (1922) 161
- [12] C. E. Chaffery, S.G. Mason, *J. Coll. Sci.* 20 (1965) 330
- [13] G. Bossis, E. Lemair, O. Volkova, H. Clercx, *J. Rheology* 41 (1997) 687
- [14] V.N. Pokrovskii, *Statistical Hydromechanics of Dilute Suspensions* (Moscow, Nauka, in Russian, 1978).
- [15] S. Ono, S. Kondo. *Molecular theory of surface tension in liquids*. (Berlin, Göttingen, Heidelberg: Springer-Verlag, 1960)
- [16] M.T. López-López, J. de Vicente, F. González-Caballero, J.D.G. Durán, *Colloids and Surfaces A: Physicochem. Eng. Aspects* 264 (2005) 75
- [17] M. T. López-López, A. Gómez-Ramírez, J. D. G. Durán, F. González-Caballero, *Langmuir* 24, (2008) 7076
- [18] M. T. Lopez-Lopez, J. de Vicente, G. Bossis, F. Gonzalez-Caballero J.D.G. Duran, *J. Mater. Res.* 20 (2005) 874.
- [19] R.M. Christensen, *Mechanics of Composite Materials*, Dover Publications, 2005
- [20] G. Batchelor, *J. Fluid Mechanics*, 46 (1971) 813
- [21] Shaqfeh, E. S. G., and G. H. Fredrickson, *Phys. Fluid A* 2, 7–24 (1990).
- [22] Larson R. G., *The Structure and Rheology of Complex Fluids* (Oxford University Press, New York, 1999), p. 353.
- [23] Férec, J., G. Ausias, M. C. Heuzey, and P. J. Carreau, *J. Rheol.* 53, 49–72 (2009).
- [24] Berthier, S., *Optique des milieux composites*, Polytechnica, Paris (1993).

### Figure capture.

Fig.1. Sketch of the model under consideration. Horizontal arrows illustrate the macroscopic velocity of suspension.

Fig.2. Illustration of the force  $f$  of the drop deformation vs. the drop aspect ratio  $r$ .

Fig.3. Total stress  $\sigma$  vs. the shear rate  $\dot{\gamma}$ . Lines represent theoretical predictions and dots the experimental data. Solid lines - calculations with (17-19), the dashed ones - by using the asymptotic estimate (20). Line 1 and open squares correspond to  $H_0=8.6$  kA/m; line 2 and black squares - to  $H_0=5.7$  kA/m. Parameters of the systems:  $\varphi_0=0.1$ ;  $\varphi_a=0.65$ ;  $\chi=70$ ;  $\eta_0=5$  mPa·s.